IOP Conference Series: Materials Science and Engineering

PAPER • **OPEN ACCESS**

Tensile properties and critical current strain limits of reinforced Bi-2212 conductors for high field magnets

To cite this article: M. Brown *et al* 2017 *IOP Conf. Ser.: Mater. Sci. Eng.* **279** 012022

View the article online for updates and enhancements.

Related content

- Making strain effects inside Bi-2212/Ag conductors visible
  Ulf Peter Trociewitz
- Toward a new paradigm in quench detection for superconducting magnets? 'Quench detection for high temperature superconductor magnets: a novel technique based on Rayleigh-backscattering interrogated optical fibers (RIOF)'
  Lucio Rossi
- Winding strain analysis for YBCO coated conductors
  W D Markiewicz and C A Swenson

This content was downloaded from IP address 146.201.225.156 on 31/01/2018 at 19:03

IOP Conf. Series: Materials Science and Engineering **279** (2017) 012022 doi:10.1088/1757-899X/279/1/012022

Tensile properties and critical current strain limits of reinforced Bi-2212 conductors for high field magnets

M. Brown[1], E. Bosque[1], D. McRae[2], R.P. Walsh[2], J. Jiang[1], E. E. Hellstrom[1], Y. Kim[1], U. Trociewitz[1], A. Otto[3], D. C. Larbalestier[1]

[1]Applied Superconductivity Center, National High Magnetic Field Laboratory, Florida State University, Tallahassee, FL 32310 USA

[2]Magnet Science & Technology Division, National High Magnetic Field Laboratory, Florida State University, Tallahassee, FL 32310 USA

[3]Solid Material Solutions, Chelmsford, MA 01863 USA

Email: mdb06h@my.fsu.edu

Abstract. We study here the effect of axial strain on the degradation of the critical current I_c for bare and reinforced, overpressure processed Bi-2212 conductors. We show that reinforcement markedly improves the conductor's stress limit, doubling it from ~150 MPa in the bare conductor to ~300 MPa when reinforced. We find also that certain processes used to reinforce the conductor slightly reduce the I_c degradation strain limit from ~0.6% to ~0.4%. Stress vs strain data taken from the samples studied here has been used to create a finite element model to explore the feasibility of using a reinforced Bi-2212 strand (produced by Solid Material Solutions) in a small test coil. The model predicts an IC limited coil with a maximum hoop strain of 0.31%, well below the experimentally verified strain limit, and is designed to lead to Bi-2212 coils that are not strain limited, but I_c limited.

1. Introduction

Bi-2212 is a high temperature superconductor (HTS) currently being developed in round wire form for use in high-field magnet applications [1] such as general purpose high-field research, nuclear magnetic resonance (NMR) [2], and the next generation of particle accelerators [3], [4]. HTS conductors are very important for operation in high fields above those attainable by the ubiquitous low temperature superconductors (LTS), Nb_3Sn and Nb-Ti. Bi-2212 is unique in that it is the only HTS conductor capable of high critical current density J_c available in a macroscopically isotropic, round-wire form. This allows for its use in well understood cabling technologies commonly used for round wire LTS like Rutherford cabling [5].

From the perspective of using Bi-2212 for high-field magnet applications, the overpressure heat treatment (OPHT) process can reliably achieve high overall wire critical current densities, J_E, in present state-of-the-art Bi-2212 strands. However, high J_E values and the desire to use Bi-2212 in high fields then focuses attention on the low elastic modulus (E = 70 GPa) and low yield strength ($\sigma_{0.02}$ < 100 MPa) of the Ag/Ag alloy matrix that sheathes the Bi-2212 filaments. This leads to strain- rather

Content from this work may be used under the terms of the Creative Commons Attribution 3.0 licence. Any further distribution of this work must maintain attribution to the author(s) and the title of the work, journal citation and DOI.
Published under licence by IOP Publishing Ltd

than I_c-limited performance in many high field solenoid designs. J_E degrades as a function of strain due to progressive fracture of the Bi-2212 filaments, making mechanical characterization of reinforced strands highly desirable in the ongoing effort to increase the stress limits of the conductor at higher fields [6]–[8]. Reinforcement methods for high field coils vary: for example, the coil as a whole, the conductor, or both can be reinforced. Here we report on reinforcement at the strand level, which involves bonding a high-strength metallic alloy strip to the broad flat faces of rectangularly rolled Bi-2212 (Figure 1) [9] in a form referred to as strengthened rectangular wire (SRW).

Presently, Bi-2212 conductors are made using the Powder-In-Tube (PIT) method [10], requiring the drawing of billets of Bi-2212 powder and Ag matrix composites into thin (0.8 – 1.3 mm diameter) wires in which the Bi-2212 powder precursor is only ~70% dense [11]. The critical current (I_c) of Bi-2212 wires can be significantly enhanced by implementing an over-pressure heat treatment (OPHT) at 10-100 bar of inert gas containing 1 bar pO_2 [12]. The OP densifies the Bi-2212 precursor in the Ag creep regime[13], and stifles the formation of gas bubbles which form from the agglomerated porosity in the filaments, obstructing the flow of current and greatly limiting I_c of the wire, especially in long length wires from which hot residual gas trapped in the pores cannot escape [14].

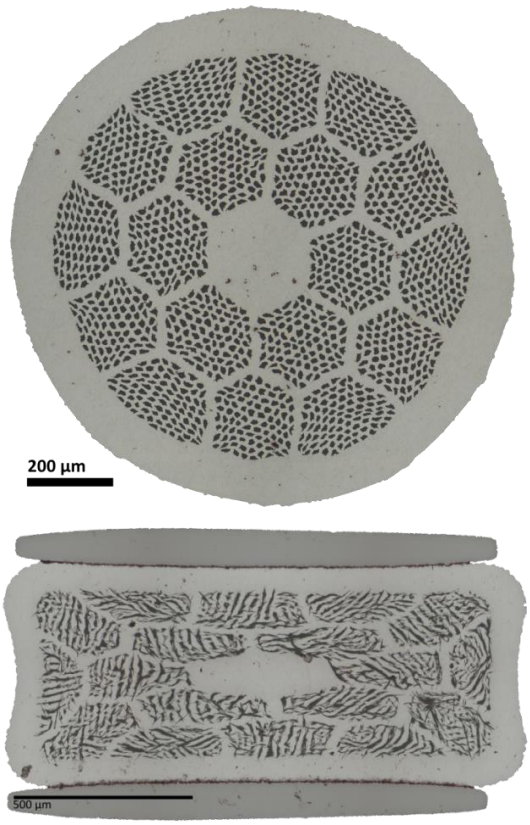

Figure 1: Transverse cross-section of a densified pmm160719-1 round wire (top) and fully heat treated strengthened rectangular wire (SRW) strand cross section; pmm160719-1 wire, rolled to a rectangular cross section and bonded to reinforcement strips on the long flat edges of the conductor (bottom).

2. Experimental Details

2.1. Bi-2212 and Ag-Mg Alloy Composite Samples

The Bi-2212 wire studied here (PMM160719-1, OST-1) was produced as a round wire by Oxford Superconducting Technologies and then made rectangular and reinforced by Solid Material Solutions (SMS). The as-delivered 1.2 mm diameter wire has a double stack, 85 x 18 filament geometry with a pure Ag matrix around each filament and an outer sheath of Ag-0.2wt%Mg alloy. During OPHT, the sheath becomes dispersion strengthened during its elevated-temperature exposure to oxygen leading to the formation of MgO_2, which provides some reinforcement for the conductor.

The wires were tested in four conditions. Some were left in the as-drawn round state, while others

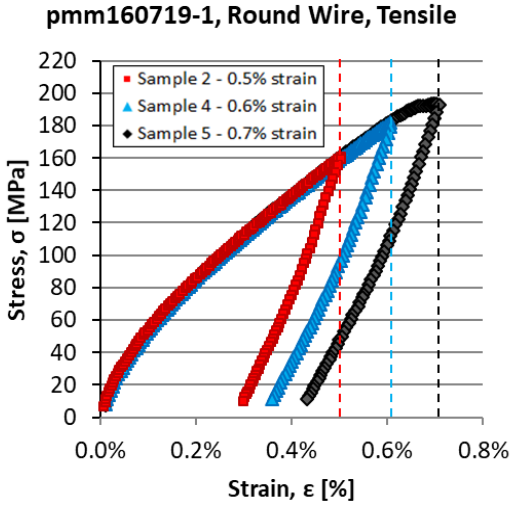

Figure 2: Stress vs. strain curves for multiple heat treated pmm160719-1 round wire samples loaded in tension each to a progressively larger strain value. One sample was left for testing I_C directly after heat treatment without any mechanical deformation.

Table 1: Geometries and mechanical properties

Sample Name	Transverse Cross Section	Reinforcement bond HT'd	Reinforced	Filament Geometry	Transverse Area [mm^2]	I_c (5T, 4.2K) [A]	J_E (5T, 4.2K) [A·mm^{-2}]	Modulus, E [GPa]
OST-1	round	no	no	85 x 18	1.083	881	814	83.6 ± 2.6
SMS-1	rectangular	no	no	85 x 18	0.643	429	667	81.7 ± 1.6
SMS-2	rectangular	yes	no	85 x 18	0.653	449	687	78.5 ± 4.3
SMS-SRW	rectangular	yes	yes	85 x 18	0.923	466	505	126 ± 3.8
SMS Laminate	flat	yes	-	-	0.120	-	-	254 ± 6.4

were rolled to a rectangular cross section. Some rectangular wires were reinforced with a strip of high strength alloy on both wide surfaces using a bonding heat treatment at 822 °C for 24 hours. Of those that were reinforced, a portion were purposefully delaminated. All samples were strained first before I_c testing. Our evaluations provide a basis to measure the effects of reshaping, reinforcing with a high strength alloy, and heat treating to secure the reinforcement to the conductor. The reinforcing material was also mechanically tested to compare to the SRWs.

All wires were over-pressure processed in argon gas containing 1 bar pO_2 at 50 bar total pressure at the NHMFL. Important sample properties are presented in Table 1.

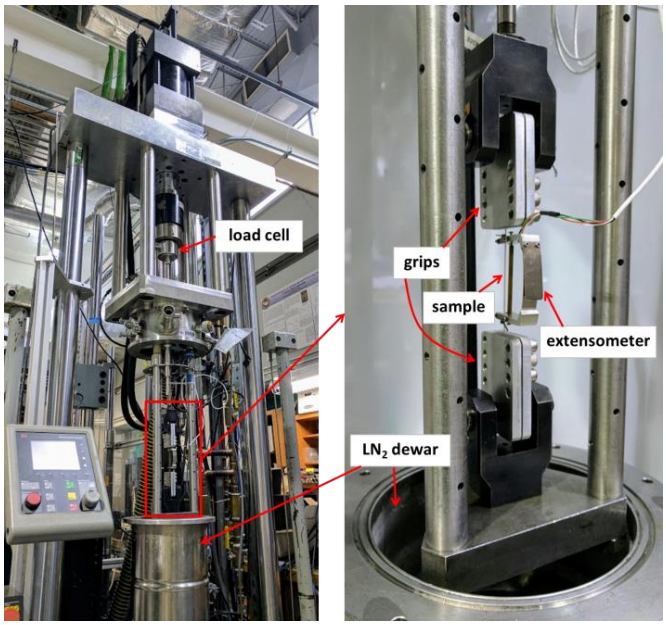

Figure 3: MTS servo-hydraulic test machine at the NHMFL, and tensile test set-up.

2.2. Stress vs. Strain

In order to measure the tensile strain dependence of I_c, the specimens were axially loaded to progressively larger strains that encompass the expected strain range of degradation. Figure 2 shows the loading sequences used for pmm160719-1 round wire, which are representative for all wires in this study. Mechanical testing was performed at the NHMFL on an MTS servo-hydraulic test machine (Figure 3) fitted with a 1kN load cell in a cryostat. Sample elongation was measured using a 50.8 mm gauge length extensometer (designed by J. Shepic) calibrated at 77 K. Samples were submerged in LN_2, and strained at a rate of 0.5 mm/min to the desired strain, at which point the sample was carefully removed for later testing and microscopy. Stress vs. strain curves were also taken separately for the reinforcement

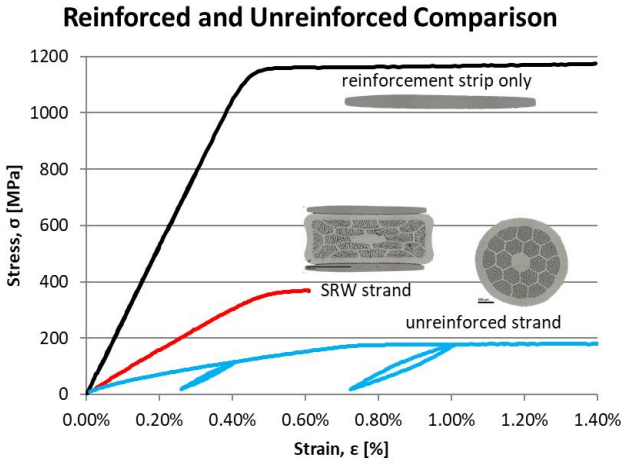

Figure 4: Stress- strain curves for reinforcement strip, reinforced OPHT SRW strand, and unreinforced OPHT pmm160719-1 round wire. All tests were performed in LN_2 at

material itself (Figure 4). The moduli reported in Table 1 are taken from unloading portions of the stress-strain curves.

2.3. Measurement of I_c

After samples had been axially loaded, they were I_c tested using the four-probe transport method in a magnetic field of 5 T at 4.2 K with a 1 $\mu V \cdot cm^{-1}$ voltage criterion. For the round wires, the magnetic field was applied perpendicular to the wire axis, and for the rectangular wires the magnetic field was applied perpendicular to the wire axis and the long flat faces. The overall critical current density for each sample, J_E, was calculated using the whole wire cross sectional area after OPHT, including the high strength laminate for strengthened wires.

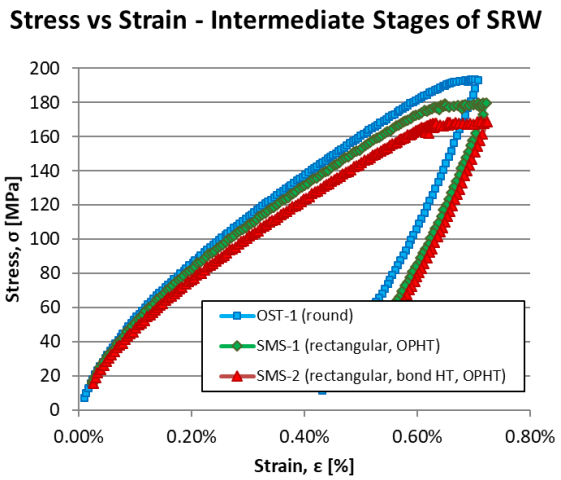

Figure 5: Stress vs. strain curves for intermediate wires in the SRW process: pmm160719-1 round wire (OPHT), the 17R1 wire rolled to rectangular cross section (OPHT), and the C67aR1 wire also rolled to rectangular cross section (bond HT & OPHT).

Cross sectional areas of the round wire were calculated using sample diameters measured over a 2cm length by an INEXiv automated digital measurement microscope. Only those wires determined to have been fully densified were used for this study. Cross sectional areas and filament area for the rectangular samples were calculated using digital images taken with an Olympus digital microscope. Samples were also imaged in a Zeiss 1540EsB Crossbeam field emission scanning electron microscope (FESEM) using a backscatter electron (BSE) detector.

3. **Results**

3.1. Stress vs Strain

The primary stress-strain data are shown in Figure 4. The unreinforced wire transitions into a constant stress deformation mode at about ~0.6% strain and 180 MPa during which the filaments break and some work-hardening of the Ag compensates the loss of strength caused by broken Bi-2212 filaments. The laminated and bonded SRW starts to yield at about 300 MPa and ~0.4% strain, while the reinforcement itself has a yield of about 1150 MPa at a strain of ~0.4%.

Figure 5 shows tensile data of wires in intermediate stages of SRW production. First we show the round wire from which all SRW wires are produced, pmm160719-1, next the 17R1 wire, which has been rolled to a rectangular cross section by SMS, and last, the C67aR1 wire after being both rolled and subjected to bonding the high strength laminate to the long edges of the conductor. The laminate was then peeled away to test the effect of the bonding HT on the properties of the conductor itself. All wires in this study, including these, were heat treated together by OPHT at 50 bar.

The data in Figure 5 show that each processing step does slightly reduce both the elastic modulus and the onset of yield. Modulus values taken from the initial slope at the point of unloading the samples can be found in Table 1. These values have ranges that may overlap, but from Figure 5 we can see that although the unloading slopes closely resemble one another, the effective moduli before first yield are clearly different. The stress at which each sample goes plastic also decreases with each additional processing step.

3.2. I_C & Limits of Strain-Induced I_C Degradation

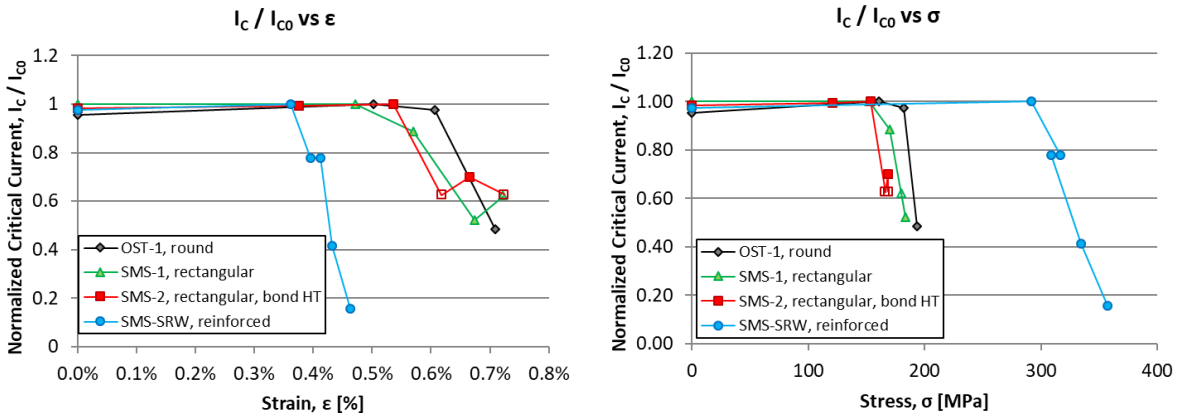

Figure 6: I_C / I_{C0} vs. strain (left) and stress (right) for each sample showing the point at which I_c begins to degrade significantly. Each data point represents one sample, strained to a defined maximum value at 77 K and then released. I_c was then tested at 4.2 K in a 5T background. It is clear the damage begins at about twice the stress in the reinforced wire but also that the critical strain is reduced from ~0.6% to ~0.4%.

Coils made from unreinforced Bi-2212 conductors will often be strain limited by fracture of the Bi-2212 filaments induced by Lorentz stresses since it has been shown that I_C degrades as strain reaches ~0.6 % in round, unreinforced strand [7]. Figure 6 shows I_C / I_{C0} vs strain (left) and stress (right) data taken for each sample type. The OST-1 round wire shows the highest strain limit slightly above 0.6 %, whereas I_C for SMS-1 and SMS-2 drops off at less than 0.6 % strain. This indicates two things: first, that rolling the conductor to rectangular shape can slightly degrade the conductor's strain limit. Second, SMS-2, having gone through a bonding HT at 820°C before OPHT, does not show a reduced strain limit, implying that, although a bond HT mildly affects the mechanical properties of the wire (Figure 5), it does not affect the strain properties of the filaments themselves. More significantly, we see a decrease in the strain limit of reinforced SMS-SRW wire from ~0.6% to ~0.4%, but Figure 6 (right) also shows that the reinforcement effectively doubles the stress at which degradation starts to occur from 150-160 MPa to ~300 MPa. This is for a wire with 21.5% reinforcement in the cross section.

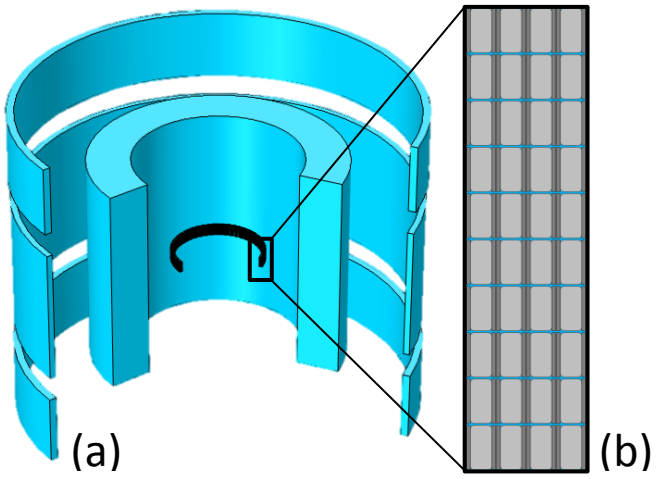

Figure 7: Cross sectional view of SRW test coil modelled using Comsol Multiphysics. (a) Large blue coils represent cryocooled LTS magnet which produces an 8 T background field. (b) The light grey regions are the conductor itself, the dark grey regions are strips of reinforcement bonded to both sides of the conductor, and the blue indicates interstitial regions filled with epoxy.

3.3. Finite Element Coil Modelling

A finite element model (FEM) of a potential Bi-2212 SRW test coil using these stress-strain data was built using Comsol Multiphysics. Figure 7 shows an axisymmetric longitudinal coil cross section built of SRWs, and depicts the proposed winding pack operating in an ~8 T

Table 2: SRW Comsol Model Parameters

Layers:	4	**Build:**	3 mm
Turns/Layer:	10	**Temp:**	4.2 K
Height:	13.5 mm	**Current:**	450 A
ID:	124 mm	**J_E:**	686 A/mm^2

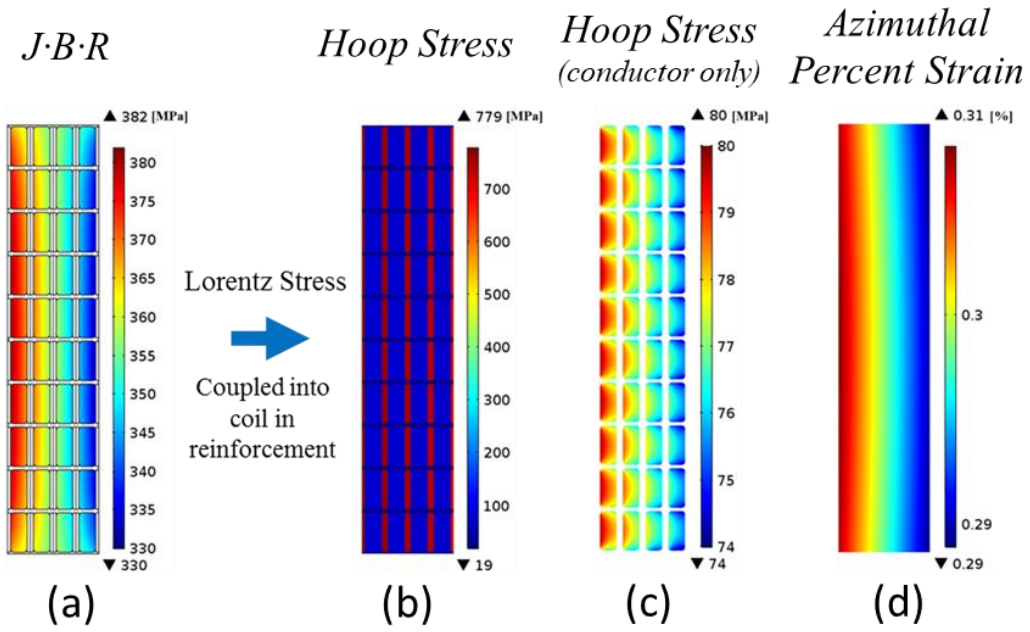

Figure 8: Coil model using an SRW-SMS simulated in Comsol Multiphysics. The figure shows (a) the calculated stress using JBR, (b) the distribution of stress within the cross section implying stress concentration in the high strength laminate, (c) the simulated final values of stress within the conductor only, and (d) the azimuthal percent strain throughout the coil cross section. Table 2 shows the coil model parameters. Note that from Tables 1 & 2, the coil is simulated very near its highest I_C value (5 T, 4.2 K), but the peak azimuthal strain (hoop strain) seen by the conductor is 0.31%, well below the 0.4% limit required to degrade I_C for SRW short samples.

background field at 4.2 K. A detailed set of test coil parameters are included in Table 2. Figure 8 (a) shows the unsupported turn $J{\cdot}B{\cdot}R$ Lorentz source averaged over the Ag/Bi-2212 conductor area (without the reinforcement) in the 8 T background field at a Ag/Bi-2212 conductor current density, J_E, of 687 A/mm^2. In this unsupported turn approximation, a peak stress of ~360 MPa occurs at the inside radius and it exceeds the maximum strength of the unreinforced wire, ~180 MPa, by about two times. However, by bonding the rectangular wire with a high strength laminate and epoxy impregnating the whole coil pack, the stress distribution is greatly changed. Figure 8 (b) reports the structural mechanical result of distributing this load between conductor and high modulus laminate, where the peak stress now reaches ~700 MPa, still well below the measured yield stress of ~1150 MPa in Figure 4. It is clear the large differences in elastic moduli concentrate stress in the reinforcing laminates. In Figure 8 (c), focus is narrowed to the Ag/Bi-2212 component alone, where the stress is everywhere less than 100 MPa, well below filament fracture stress. Finally, the resultant azimuthal strains are shown in Figure 8 (d) and they are everywhere less than 0.31%, well below the onset strain of fracture of 0.4% shown in Figure 4. In summary, when ramped to 450 A (just above the expected I_C for SRWs at 8 T) the coil is now I_C, rather than strain limited.

4. Discussion

The results presented here modelling the use of the conductor in a comparatively large bore (124 mm) test bed shows the huge value of laminating weak Ag-sheathed Bi-2212 conductors with a laminate with three times the modulus of Ag (250 vs. 70 GPa). Lamination with just 20% of the cross-section doubles the fracture strength of the conductor before filament fracture to more than 300 MPa by reducing the stress on the Ag/Bi-2212 components of the conductor. The process for lamination is flexible, allowing greater or lesser amounts to be applied, thus making this a versatile technique for controlling damage in high field Bi-2212 solenoid magnets.

5. Conclusion

This study used mechanical testing and measurement of I_C to compare the coupled mechanical and electrical properties of reinforced Bi-2212 conductor. We found that the conductor stress limits could be doubled from ~150 MPa in bare wires to 300 MPa in reinforced wires with only ~20% of laminate. Simulation of the value of the high modulus laminated conductor for a test coil showed its strong value for reducing strain on the Bi-2212 filaments in an impregnated winding.

6. Acknowledgements

We gratefully acknowledge the help of technical staff, A. Francis and G. Bradford. Additionally, we are thankful to D. Abraimov for his constant willingness for enlightening discussion.

This work was supported by a grant from the US Department of Energy, Office of High Energy Physics (DE-SC0010421) and from the NHMFL, which is supported by the NSF under NSF/DMR-1157490 and by the State of Florida. Research reported in this publication was also supported by the National Institute of General Medical Sciences of the National Institutes of Health under Award Number R21GM111302. The content is solely the responsibility of the authors and does not necessarily represent the official views of the National Institutes of Health.

References

[1] Y. Huang, H. Miao, S. Hong, and J. A. Parrell, "Bi-2212 Round Wire Development for High Field Applications," *IEEE Trans. Appl. Supercond.*, vol. 24, no. 3, pp. 1–5, Jun. 2014.
[2] H. W. Weijers *et al.*, "High Field Magnets With HTS Conductors," *IEEE Trans. Appl. Supercond.*, vol. 20, no. 3, pp. 576–582, Jun. 2010.
[3] A. Godeke *et al.*, "Wind-and-react Bi-2212 coil development for accelerator magnets," *Supercond. Sci. Technol.*, vol. 23, no. 3, p. 34022, 2010.
[4] A. Ballarino, "Prospects for the use of HTS in high field magnets for future accelerator facilities," *CERN Document Server*, 11-Nov-2014. [Online]. Available: http://cds.cern.ch/record/1968557. [Accessed: 15-Jun-2017].
[5] E. Barzi, V. Lombardo, D. Turrioni, F. J. Baca, and T. G. Holesinger, "BSCCO-2212 Wire and Cable Studies," *IEEE Trans. Appl. Supercond.*, vol. 21, no. 3, pp. 2335–2339, Jun. 2011.
[6] A. Godeke *et al.*, "Critical current of dense Bi-2212 round wires as a function of axial strain," *Supercond. Sci. Technol.*, vol. 28, no. 3, p. 32001, Mar. 2015.
[7] R. Bjoerstad *et al.*, "Strain induced irreversible critical current degradation in highly dense Bi-2212 round wire," *Supercond. Sci. Technol.*, vol. 28, no. 6, p. 62002, 2015.
[8] U. P. Trociewitz, "Making strain effects inside Bi-2212/Ag conductors visible," *Supercond. Sci. Technol.*, vol. 28, no. 7, p. 70501, 2015.
[9] A. Otto, "Reinforced 2212 multifilament superconducting wire with low aspect shape, cables thereof, and 2223 silver tape-based cables," WO2016130975 A2, 18-Aug-2016.
[10] H. Miao, K. R. Marken, M. Meinesz, B. Czabaj, and S. Hong, "Development of round multifilament Bi-2212/Ag wires for high field magnet applications," *IEEE Trans. Appl. Supercond.*, vol. 15, no. 2, pp. 2554–2557, Jun. 2005.
[11] J. Jiang *et al.*, "Doubled critical current density in Bi-2212 round wires by reduction of the residual bubble density," *Supercond. Sci. Technol.*, vol. 24, no. 8, p. 82001, Jun. 2011.
[12] D. C. Larbalestier *et al.*, "Isotropic round-wire multifilament cuprate superconductor for generation of magnetic fields above 30 T," *Nat. Mater.*, vol. 13, no. 4, pp. 375–381, Apr. 2014.
[13] T. Shen, A. Ghosh, L. Cooley, and J. Jiang, "Role of internal gases and creep of Ag in controlling the critical current density of Ag-sheathed $Bi_2Sr_2CaCu_2O_x$ wires," *J. Appl. Phys.*, vol. 113, no. 21, p. 213901, Jun. 2013.
[14] F. Kametani *et al.*, "Bubble formation within filaments of melt-processed Bi2212 wires and its strongly negative effect on the critical current density," *Supercond. Sci. Technol.*, vol. 24, no. 7, p. 75009, 2011.

[15] A. Kajbafvala, W. Nachtrab, R. Kumar, F. Hunte, T. Wong, and J. Schwartz, "High strength oxide dispersion strengthened silver aluminum alloys optimized for $Bi_2Sr_2CaCu_2O_x$ round wire," *Supercond. Sci. Technol.*, vol. 26, no. 12, p. 125012, 2013.
[16] A. Kajbafvala, W. Nachtrab, T. Wong, and J. Schwartz, "$Bi_2Sr_2CaCu_2O_x$ round wires with Ag/Al oxide dispersion strengthened sheaths: microstructure–properties relationships, enhanced mechanical behavior and reduced Cu depletion," *Supercond. Sci. Technol.*, vol. 27, no. 9, p. 95001, 2014.
[17] M. Matras, "Investigation of Ag-sheathed multi-filamentary $Bi_2Sr_2CaCu_2O_x$ superconducting round wires processed with overpressure, for high field magnets," PhD thesis, Materials Science Program, The Florida State University, 2016.